# Approaches to Mitigate Edge Recombination Effects in Silicon Lifetime Samples With Emitter

David Bäurle, Axel Herguth, and Giso Hahn

***Abstract*—Insufficiently sized symmetric lifetime samples with pn-junction exhibit a specific injection-dependent effective charge carrier lifetime measured by photoconductance decay due to increased edge recombination, characterized by a strong decline toward low injection. In this study, various approaches are presented to suppress these edge effects in n-type Si samples with boron emitter. These approaches include edge passivation using $AlO_x$ from atomic layer deposition and the creation of an undiffused buffer layer between the central measurement area and recombination-active edges. For the latter, both an etch-back approach and a masked diffusion of the boron emitter (sunken emitter) are evaluated. Lifetime measurements and photoluminescence imaging demonstrate that the sunken emitter approach most effectively suppresses edge recombination in small-sized lifetime samples.**

***Index Terms*—Crystalline silicon, edge passivation, edge recombination, injection-dependent excess charge carrier lifetime.**

## I. Introduction

THE injection-dependent lifetime is a key parameter describing the suitability of silicon material and passivation layers for use in solar cells, as it reflects all different recombination channels (intrinsic, bulk defects, and surface) in a "global way." In an ideal case their specific injection-dependent contribution to recombination can be used to separate their influence and to extract characteristic quantities. Commonly this is done by photoconductance decay (PCD) measurements yielding a spatially integrated lifetime in dependence of carrier injection $\tau_{\mathrm{eff}}(\Delta n)$ within a sensitivity region. However, this only works reliably if excess charge carriers are lost by recombination within this sensitivity region and not by transport out of this region. Hence, regions of different recombination activity, such as unpassivated sample edges, have to be "sufficiently" far away from the sensitivity region. Commonly, the diffusion length of minority carriers is thought to define this length scale, however, lifetime samples with an inversion layer are known to exhibit increased edge recombination even if edges are further away than a few diffusion lengths, strongly limiting $\tau_{\mathrm{eff}}(\Delta n)$ in low injection. In this context, an inversion layer is to be understood as a surface layer in which bulk minority carriers become majority carriers and vice versa. It may stem from field-effect passivation—such as for negatively charged $AlO_x$ on n-type Si—or from a pn-junction created by a classical emitter diffusion or passivating contacts structures, such as n-type poly-Si on a p-type base or vice versa. The reason for this behavior is that the inversion layer provides an efficient transport channel for minority carriers, thereby allowing edge recombination to influence regions further from the sample edges [1], [2], [3].

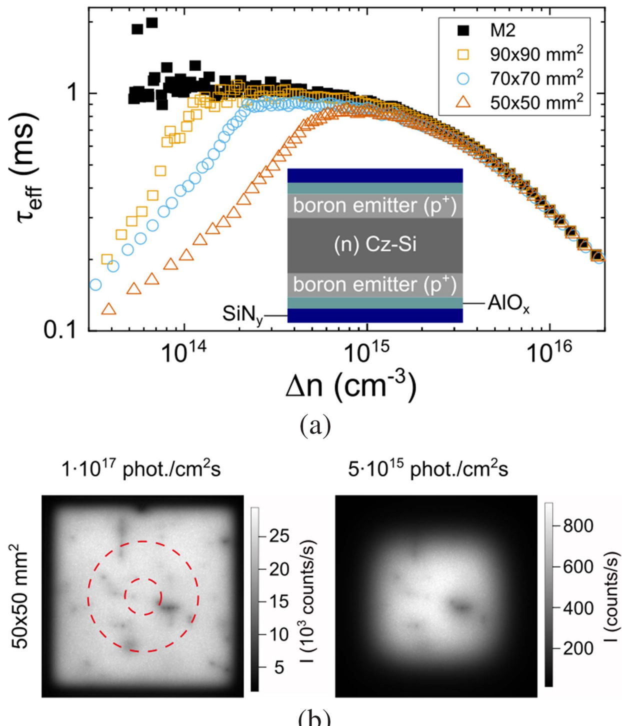


Fig. 1. (a) Influence of edge recombination on injection-dependent $\tau_{\mathrm{eff}}(\Delta n)$ curves measured at the sample center using the Sinton lifetime tester (WCT-120) for differently sized samples with pn-junction and unpassivated edges. (b) PL images of the corresponding $50 \times 50\ \mathrm{mm}^2$ sample recorded at different excitation.

The impact of edge recombination on $\tau_{\mathrm{eff}}(\Delta n)$ is illustrated in Fig. 1 showing the results from transient PCD measurements done with a WCT-120 lifetime tester from Sinton Instruments [4]. The ring-like sensitivity region is highlighted in Fig. 1(b) as the area between the two dashed red circles. Shown is the region where the sensitivity coefficient determined by numerical simulations in [5] is above 10% of its maximum value leading to an outer diameter of 27 mm.

An n-type Cz-Si sample with a boron emitter is successively reduced in size from M2 format ($156.75 \times 156.75\ \mathrm{mm}^2$) using

Received 4 April 2025; accepted 30 April 2025. Date of publication 23 May 2025; date of current version 20 June 2025. This work was supported by the German Federal Ministry of Economic Affairs and Climate Action under Grant 03EE1176C. *(Corresponding author: David Bäurle.)*

The authors are with the Department of Physics, University of Konstanz, 78457 Konstanz, Germany (e-mail: david.baeurle@uni-konstanz.de; axel.herguth@uni-konstanz.de; giso.hahn@uni-konstanz.de).

Digital Object Identifier 10.1109/JPHOTOV.2025.3568471

2156-3403 © 2025 IEEE. All rights reserved, including rights for text and data mining, and training of artificial intelligence and similar technologies.
Personal use is permitted, but republication/redistribution requires IEEE permission. See https://www.ieee.org/publications/rights/index.html for more information.

*Konstanzer Online-Publikations-System (KOPS)*
*URL: http://nbn-resolving.de/urn:nbn:de:bsz:352-2-119iibd6yp87y5*

laser cutting which creates unpassivated edges. This leads to an increasing injection range being dominated by edge recombination related effects [see Fig. 1(a)]. For a sample size of $50 \times 50\ \mathrm{mm}^2$, $\tau_{\mathrm{eff}}(\Delta n < 10^{15}\ /\mathrm{cm}^{-3})$ is significantly limited. Consequently, the analysis of such edge-impacted $\tau_{\mathrm{eff}}(\Delta n)$ curves is prone to error and misinterpretation, in particular toward low injection. The fact that this effect originates from unpassivated edges is evident from the photoluminescence (PL) images in Fig. 1(b). The two images were recorded under different excitation conditions, corresponding to higher and lower injection levels, respectively. While at a photon flux of $1 \times 10^{17}\ \mathrm{phot./\,cm^2\,s}$ only a small edge-adjacent region exhibits low luminescence and the sensitivity region is well within the homogeneous center, the low-luminescence regions extend further into the sample at a lower photon flux of $5 \times 10^{15}\ \mathrm{phot./\,cm^2\,s}$.

The problems caused by increased edge recombination only arise when large processed samples (in this case, M2 format) are subsequently downsized. In addition to the decreasing sample size, the newly created laser-cut edges remain in most cases unpassivated. This reduces the distance between the measurement region at the center of the sample and the edges while increasing the recombination velocity at the latter. While a large sample might be a simple solution for one-shot studies, long-term (light-induced) degradation studies tremendously benefit from parallelization made possible by small samples. Performing all processing steps ($BBr_3$ diffusion, deposition of passivation layers, and fast-firing) on small wafers should lead to well passivated edges but often goes along with handling marks within the PCD's sensitivity region. Also, process-related inhomogeneities owing, e.g., to the dynamic firing process in belt furnaces [6] can be avoided by selecting a rather homogeneous part of the sample (usually close to the center) for further studies. Thus, samples are typically processed on larger size before being cut to the final size.

The challenges posed by increased edge recombination caused by newly formed unpassivated edges are also well known in other areas of solar cell research. During the fabrication of solar modules from half-cut [7] or even shingled cells [8], [9], fully processed, metallized, and fired solar cells are subsequently cut to smaller size to achieve primarily electrical benefits during interconnection. In this context, edge passivation becomes a critical challenge as increased edge recombination due to the existance of a pn-junction directly at the unpassivated edges leads to lower $V_{oc}$ and pseudo fill factor [8]. A common approach employed to mitigate this difficulty involves a preferably damage-free separation of the cells followed by passivation with atomic layer deposition (ALD) $AlO_x$ [8], [9]. The $AlO_x$ provides chemical passivation of the exposed edges, complemented by field-effect passivation due to the formation of negative charges within the layer [10]. Alternatively, an emitter window can be created to ensure that no emitter (nor inversion layer) is present in the region where the cell will later be separated, thereby preventing an open pn-junction at the newly formed edge [11], [12].

In this study, comparable approaches were applied in the context of lifetime samples. The edge passivation quality of the resulting samples is evaluated based on how effectively the lifetime limitation in low injection can be suppressed in, otherwise, similarly processed lifetime samples.

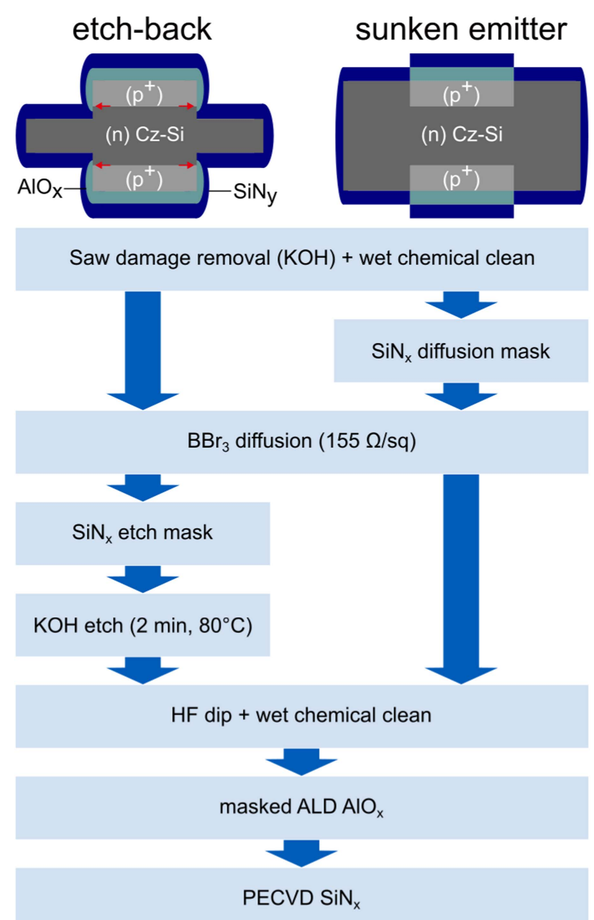


Fig. 2. Process flow for the *etch-back* and *sunken emitter* approaches.

## II. Experimental

All samples presented in this work were processed using phosphorous-doped M2 n-type Cz-Si wafers with a resistivity of 2 to 3 Ωcm. The boron emitter with an average sheet resistance of $155\ \Omega/\mathrm{sq}$ was formed by $BBr_3$ diffusion. As a reference, samples with laser cut and thus completely unpassivated edges were prepared. In addition, three alternative approaches were utilized to presumably reduce edge recombination.

For the *cleave-and-passivate* approach a wafer was cleaved to the final size ($50 \times 50\ \mathrm{mm}^2$) by a diamond tip scribe at the edge, followed by a slight wafer bending which propagates the crack through the sample. This should lead to comparably smooth and uniform edges introducing less damage compared to laser cutting [9], [13]. Following the cleavage, a $25\ \mathrm{nm}$ thick $AlO_x$ deposited by ALD is annealed for $30\ \mathrm{min}$ at $400\ ^\circ\mathrm{C}$ to passivate the sample's surfaces including the newly formed edges.

Applying an emitter window for edge passivation is achieved through two different approaches with sample preparation summarized in Fig. 2. The *etch-back* approach utilizes a masked etch-back of the boron emitter in KOH in the outer parts of the sample whereas the *sunken emitter* approach confines the emitter

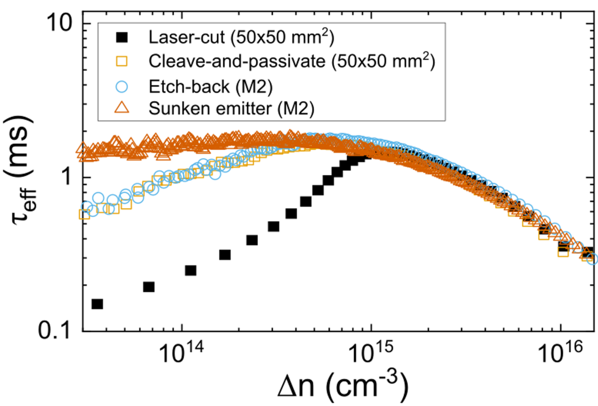


Fig. 3. Injection-dependent $\tau_{\text{eff}}(\Delta n)$ curves for samples with varying degrees of edge passivation. A $50 \times 50\ \text{mm}^2$ sample with laser-cut, unpassivated edges (black squares) is compared to a sample cleaved with a diamond scribe and passivated with ALD $AlO_x$ (*cleave-and-passivate*, amber squares). Also shown are samples processed using the *etch-back* (blue circles) and *sunken emitter* (rust triangles) approaches. The emitter area of the latter two also measures $50 \times 50\ \text{mm}^2$, while the full sample corresponds to M2 size.

to a restricted central area by applying a diffusion mask prior to emitter formation. In both cases a plasma-enhanced chemical vapor deposition $SiN_x$ is used as mask, which was deposited using the corresponding shadow masks laser cut from Si wafers. The resulting structures are passivated by an $AlO_x/SiN_y$ stack on the emitter area again by suitable masking. The undiffused sample borders are solely passivated by $SiN_x$ to prevent increased edge recombination due to inversion passivation. As all masked processing steps are the result of placing shadow masks on the samples no rigorously perfect alignment can be guaranteed. Small misalignments between $AlO_x$ and boron emitter cannot be excluded, which would lead to partly covered emitter regions with only $SiN_x$ and undiffused regions with an $AlO_x/SiN_y$ stack, respectively. Afterward, a firing step was carried out in a belt furnace with a peak sample temperature of $T_{\text{peak}} = 750\ ^\circ\text{C}$ to activate surface passivation.

## III. Results and Discussion

In the following section, the level of edge passivation of the four differently processed sample types is compared by means of injection-dependent lifetime measurements. The *etch-back* and *sunken emitter* approaches aim for the potential to reduce sample size post hoc—after processing—without introducing an increased influence of edge-recombination to the PCD measurements. So, the influence on $\tau_{\text{eff}}(\Delta n)$ curves of subsequently reducing sample size by laser cutting is investigated for the two approaches. In addition, effects of potential misalignments between passivation layers and emitter are investigated by deliberately using unfitting shadow masks during $AlO_x$ deposition.

### A. Level of Edge Passivation

The injection-dependent $\tau_{\text{eff}}(\Delta n)$ curves of the differently processed samples are shown in Fig. 3. For the $50 \times 50\ \text{mm}^2$ laser cut sample the injection range below $\Delta n = 10^{15}\text{cm}^{-3}$ is strongly limited due to edge-related recombination.

This limitation is reduced but still visible for the $50 \times 50\ \text{mm}^2$ sample with $AlO_x$ edge passivation, which still seems to suffer from insufficiently passivated edges despite the $AlO_x$ layer. In contrast, the *sunken emitter* sample still being in M2 format does not show any limitation toward low injection. Even if edge recombination would be an issue, the edges are likely too far from the measurement region, especially due to the missing inversion layer in the undiffused part of the sample. Interestingly, the *etch-back emitter* sample shows limitations toward low injection despite being in M2 format as well.

The decisive difference between the *etch-back* and *sunken emitter* approach is the creation of new edges around the emitter area during etch-back that are marked with red arrows in Fig. 2. Although these new edges with a depth of less than 5 $\mu$m only make up a small proportion of the entire edges, they contain the space charge region (SCR) of the pn-junction where the recombination rate is highest [2], [14], [15]. Those new edges are passivated during the depositions of the $AlO_x/SiN_y$ stack. Consequently, the *etch-back* approach leads to similar conditions as the edge passivation with ALD $AlO_x$ on the $50 \times 50\ \text{mm}^2$ cleaved sample resulting in almost identical injection-dependent $\tau_{\text{eff}}(\Delta n)$. The lifetime limitations toward low injection in both cases are reduced but not completely suppressed due to insufficient passivation.

However, it remains an open question why exactly the *sunken emitter* approach shows superiority to the *etch-back* or the *cleave-and-passivate* approach. Unlike the latter two where etching and cleaving results in a vertical cut of the diffused emitter and the SCR, the *sunken emitter* should correspond to a horizontal cut where boron diffused laterally underneath the diffusion mask. In both cases, the same $AlO_x/SiN_x$ stack should be present, thus both cases should probably show a similar behavior. However, it seems that there is still a significant difference granting superiority to the *sunken emitter* approach. It might be related to the exact shape of the boron profile underneath the diffusion mask, and how the passivation layers form and interact with the substrate on a microscopic scale.

### B. Influence of Sample Size Reduction

As it is the aim of the *etch-back* and the *sunken emitter* approach to allow for size reduction after processing, this is studied in detail in the following by laser cutting these samples without any subsequent edge passivation. Corresponding $\tau_{\text{eff}}(\Delta n)$ curves are shown in Fig. 4. For both approaches, the shape of $\tau_{\text{eff}}(\Delta n)$ remains unchanged as long as the remaining distance between the emitter region and the newly formed edges is large enough (shown for distances of at least $5\ \text{mm}$ with the $70 \times 70\ \text{mm}^2$ and $60 \times 60\ \text{mm}^2$ sample, respectively). Once the emitter is in contact with the newly formed edges, limitations of $\tau_{\text{eff}}(\Delta n)$ arise in low injection from increased edge recombination. Hence, both approaches seem to effectively disrupt the transport channel of the minority carriers toward the recombination-active laser cut (outer) edges in the nondiffused area. This prevents any influence on $\tau_{\text{eff}}(\Delta n)$ of the recombination occurring there.

This finding is also supported by PL images captured at two distinct excitation levels illustrated in Fig. 5. Here, samples are shown utilizing the *sunken emitter* approach with a $50 \times 50\ \text{mm}^2$ emitter area located within the red marks. The

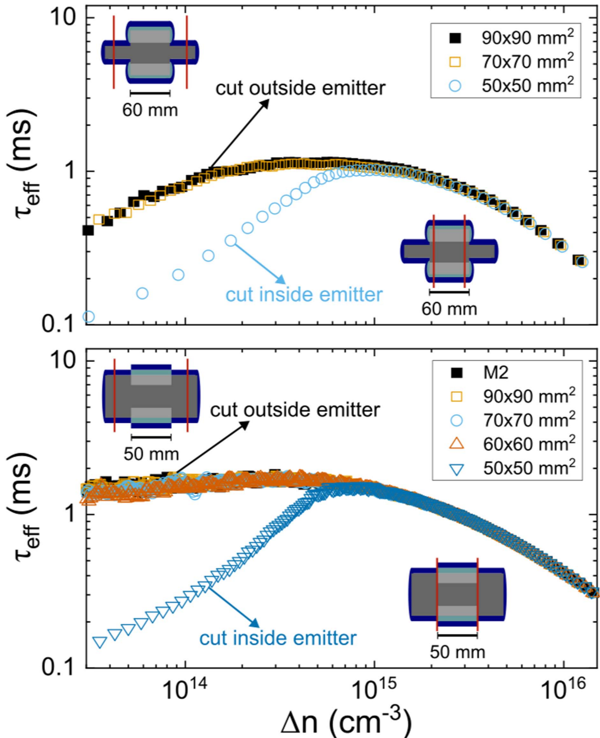


Fig. 4. Injection-dependent lifetime curves of laser-cut samples processed on M2 size using the (top) *etch-back* and (bottom) *sunken emitter* approach.

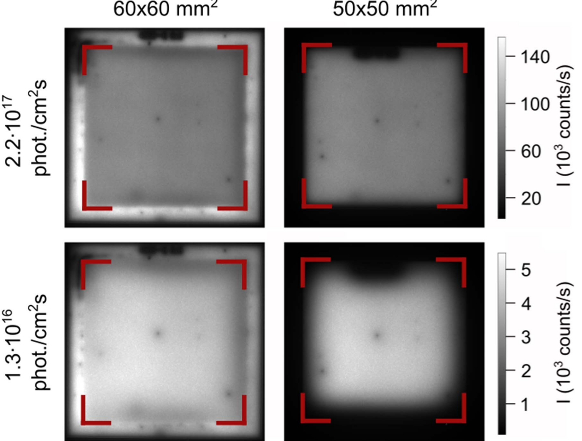


Fig. 5. PL images captured at two distinct excitation levels for the $60 \times 60\ \mathrm{mm}^2$ and $50 \times 50\ \mathrm{mm}^2$ *sunken emitter* samples, corresponding to the $\tau_{\mathrm{eff}}(\Delta n)$ curves shown in the bottom of Fig. 4. The emitter area lies within the red squares which corresponds to the complete $50 \times 50\ \mathrm{mm}^2$ sample.

sample on the left has an edge length of $60\ \mathrm{mm}$, which results in an undiffused frame of $5\ \mathrm{mm}$ width between emitter area and edges. The same sample was laser cut to $50 \times 50\ \mathrm{mm}^2$ resulting in direct contact between emitter and edges. PL images of this case are shown on the right of Fig. 5. While the luminescence of the $50 \times 50\ \mathrm{mm}^2$ sample is hardly reduced toward the edges for high excitation (rather high injection), it is strongly reduced for lower excitation (rather low injection) reflecting the limitation in $\tau_{\mathrm{eff}}(\Delta n)$ shown in the bottom part of Fig. 4. In contrast, the $5\ \mathrm{mm}$ wide frame without emitter limits the hole transport to the

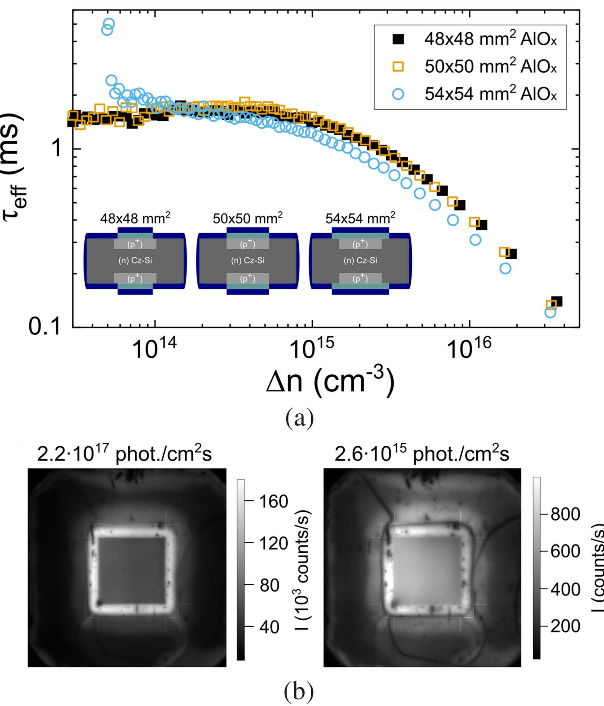


Fig. 6. (a) Injection-dependent lifetime curves of samples prepared with misalignment between $\mathrm{AlO_x}$ and emitter region. (b) PL images of the corresponding $54 \times 54\ \mathrm{mm}^2$ sample recorded with low and high excitation.

edges and consequently the impact of edge recombination for the $60 \times 60\ \mathrm{mm}^2$ sample. Even for low excitation no strongly reduced luminescence toward the edges is visible. Hence, the *sunken emitter* approach seems to be the best choice to reduce the impact of edge recombination in the presented small lifetime samples with boron emitters.

## C. Impact of Passivation Layer Alignment

As already mentioned in section II, a potential misalignment between emitter region and $\mathrm{AlO_x}$ deposition can arise during sample preparation with emitter window, which may lead to varying conditions at the surface-adjacent pn-junction. How this might influence resulting *sunken emitter* samples was investigated by deliberately depositing an $\mathrm{AlO_x}$ layer with deviating size on the $50 \times 50\ \mathrm{mm}^2$ emitter region. During the $\mathrm{AlO_x}$ deposition shadow masks with $48 \times 48\ \mathrm{mm}^2$ and $54 \times 54\ \mathrm{mm}^2$ openings were used to aim at samples where the lateral pn-junction is passivated by solely $\mathrm{SiN_x}$ and by an $\mathrm{AlO_x/SiN_y}$ stack, respectively. The injection-dependent lifetime curves of those samples are shown in Fig. 6(a). It can be seen that depositing the $\mathrm{AlO_x}$ with a shadow mask slightly smaller than the emitter region does not seem to have an impact on $\tau_{\mathrm{eff}}(\Delta n)$. However, if the $\mathrm{AlO_x}$ is deposited on a considerably larger area than the emitter ($2\ \mathrm{mm}$ on all sides), a distortion of the lifetime curve toward low injection becomes visible. Opposing to the limitation caused by the effect of edge recombination, an abrupt rise in effective lifetime can be observed for the corresponding sample. The $\mathrm{AlO_x/SiN_y}$ passivation on the undiffused surface is superior to both the emitter region with stack passivation as well as the

undiffused region passivated solely by $SiN_x$. The resulting higher effective lifetime, which can be seen by increased luminescence in the PL images as shown in Fig. 6(b), leads to a reservoir of minority carriers that are connected to the measurement area by the present inversion layers (inversion passivation and emitter). With ongoing measurement time these holes can travel to the measurement area with emitter to recombine, which influences the measured conductivity, and therefore the apparent effective lifetime in low injection is increased. In the PL image recorded at low excitation an expanding of the high luminescence region can be seen, which indicates that indeed recombination characteristics outside the actual measurement area are impacting the latter. Accordingly, it should be avoided to create areas with strongly varying surface passivation in close proximity of the emitter region especially if an efficient minority carrier transport channel (in this case due to field effect passivation) is present as well. However, the resulting lifetime curves of the *sunken emitter* approach seem to be quite stable toward small misalignments.

## IV. Conclusion

Lifetime samples with pn-junction exhibit strong injection-dependent $\tau_{\text{eff}}(\Delta n)$ curves toward low injection when cut to $50 \times 50\ \text{mm}^2$ as edge recombination impacts the sensitivity region during PCD measurements. The *cleave-and-passivate* approach, which utilizes a mechanical cleaving introducing less damage than the laser cut and a subsequent edge passivation by ALD $AlO_x$ leads to reduced but still noticeable edge recombination related lifetime limitations in low injection. It seems that edge passivation with $AlO_x$ is not suited to suppress the effects of edge recombination completely.

Both emitter window approaches succeed in decoupling the edges created by laser cutting in the undiffused area from the measurement area in the emitter region. However, $\tau_{\text{eff}}(\Delta n)$ curves of *etch-back* samples still show an almost identical injection-dependence as with the *cleave-and-passivate* approach. Here, new (inner) edges are formed during the etch-back, which are passivated by $AlO_x/SiN_y$ causing similar conditions with insufficiently passivated vertical edges including the SCR. The *sunken emitter* approach leads to superior edge passivation. For the shown samples any lifetime limitations in low injection are suppressed successfully. Although regions with strongly deviating recombination characteristics close to the emitter region are shown to distort the $\tau_{\text{eff}}(\Delta n)$ curves in low injection as well, minor process-related misalignments between emitter and $AlO_x$ can be tolerated without noticeable effects.

## Acknowledgment

The authors would like to thank Bärbel Rettenmaier for technical support. The content is the responsibility of the authors.

## References

[1] B. Veith et al., "Injection dependence of the effective lifetime of n-type Si passivated by $Al_2O_3$: An edge effect?," *Sol. Energy Mater. Sol. Cells*, vol. 120, pp. 436–440, Jan. 2014.

[2] M. Kessler, T. Ohrdes, P. P. Altermatt, and R. Brendel, "The effect of sample edge recombination on the averaged injection-dependent carrier lifetime in silicon," *J. Appl. Phys.*, vol. 111, no. 5, Mar. 2012, Art. no. 054508.

[3] R. Basnet et al., "Understanding the strong apparent injection dependence of carrier lifetimes in doped polycrystalline silicon passivated wafers," *Sol. RRL*, vol. 8, no. 12, May 2024, Art. no. 2400087.

[4] R. A. Sinton and A. Cuevas, "Contactless determination of current–voltage characteristics and minority-carrier lifetimes in semiconductors from quasi-steady-state photoconductance data," *Appl. Phys. Lett.*, vol. 69, no. 17, pp. 2510–2512, Oct. 1996.

[5] L. E. Black and D. H. Macdonald, "Accounting for the dependence of coil sensitivity on sample thickness and lift-off in inductively coupled photoconductance measurements," *IEEE J. Photovolt.*, vol. 9, no. 6, pp. 1563–1574, Nov. 2019.

[6] J. Simon et al., "Correlation study between LeTID defect density, hydrogen and firing profile in Ga-doped crystalline silicon," *Sol. Energy Mater. Sol. Cells*, vol. 260, Sep. 2023, Art. no. 112456.

[7] J. Schneider, S. Schoenfelder, S. Dietrich, and M. Turek, "Solar module with half size solar cells," in *Proc. 29th Eur. Photovolt. Sol. Energy Conf. Exhib.*, 2014, pp. 185–189.

[8] P. Baliozian et al., "Postmetallization "passivated edge technology" for separated silicon solar cells," *IEEE J. Photovolt.*, vol. 10, no. 2, pp. 390–397, Mar. 2020.

[9] B. Martel, M. Albaric, S. Harrison, F. Dhainaut, and T. Desrues, "Addressing separation and edge passivation challenges for high efficiency shingle heterojunction solar cells," *Sol. Energy Mater. Sol. Cells*, vol. 250, Jan. 2023, Art. no. 112095.

[10] B. Hoex, S. B. S. Heil, E. Langereis, M. C. M. van de Sanden, and W. M. M. Kessels, "Ultralow surface recombination of *c*-Si substrates passivated by plasma-assisted atomic layer deposited $Al_2O_3$," *Appl. Phys. Lett.*, vol. 89, Jul. 2006, Art. no. 042112.

[11] S. Glunz et al., "High-efficiency silicon solar cells for low-illumination applications," in *Proc. Rec. 29th IEEE Photovolt. Specialists Conf. 2002*, 2002, pp. 450–453.

[12] K. Rühle, M. K. Juhl, M. D. Abbott, L. M. Reindl, and M. Kasemann, "Impact of edge recombination in small-area solar cells with emitter windows," *IEEE J. Photovolt.*, vol. 5, no. 4, pp. 1067–1073, Jul. 2015.

[13] J. Lelièvre et al., "Alternative CZ ingot squaring and half-cell cutting methodology for low-temperature PV cell and module technologies," in *Proc. 37th Eur. Photovolt. Sol. Energy Conf. Exhib.*, 2020, pp. 487–489.

[14] P. P. Altermatt, A. G. Aberle, J. Zhao, A. Wang, and G. Heiser, "A numerical model of p–n junctions bordering on surfaces," *Sol. Energy Mater. Sol. Cells*, vol. 74, no. 1–4, pp. 165–174, Oct. 2002.

[15] A. Fell et al., "Modeling edge recombination in silicon solar cells," *IEEE J. Photovolt.*, vol. 8, no. 2, pp. 428–434, Mar. 2018.